A.1.2 Preamplifiers

Since the noise figure of most commercially available spectrum analyzers is considerably higher than that of radio receivers, a preamplifier is used between the filter and the spectrum analyzer. Unfortunately, the low-cost preamplifiers that are commonly available have insufficient dynamic range to cope with total signal power applied to them during signal reception under the conditions encountered at most receiving facilities. The saturation of such amplifiers always results in the generation of intermodulation products and broad-band intermodulation noise. To avoid this problem, high-dynamic-range preamplifiers were provided for each radio band. The maximum total signal power at the input to each preamplifier is carefully examined prior to recording data to ensure that linear operation is achieved.

Figure 61 shows an example of a preamplifier and its power supply that is used for measurements in the HF band. The components are mounted on a large heat sink to dissipate the heat generated by the preamplifier.

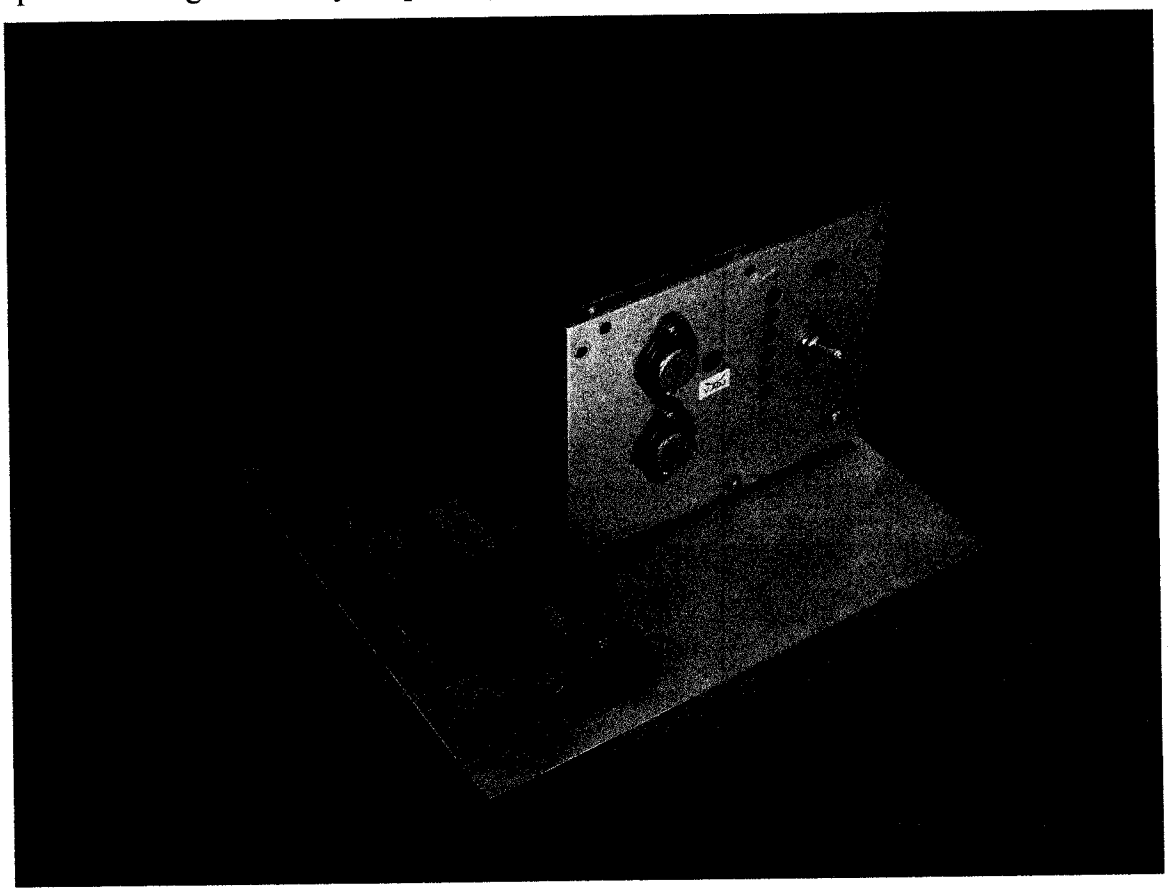

Figure 61 Example of a Preamplifier for the HF Band

Figure 62 shows an example of a preamplifier and its power supply used for the examination of signals, noise and interference in the UHF band. In this particular case sufficient heat dissipation from heat generated by the preamplifier was achieved by its heat sink and the aluminum mounting plate.

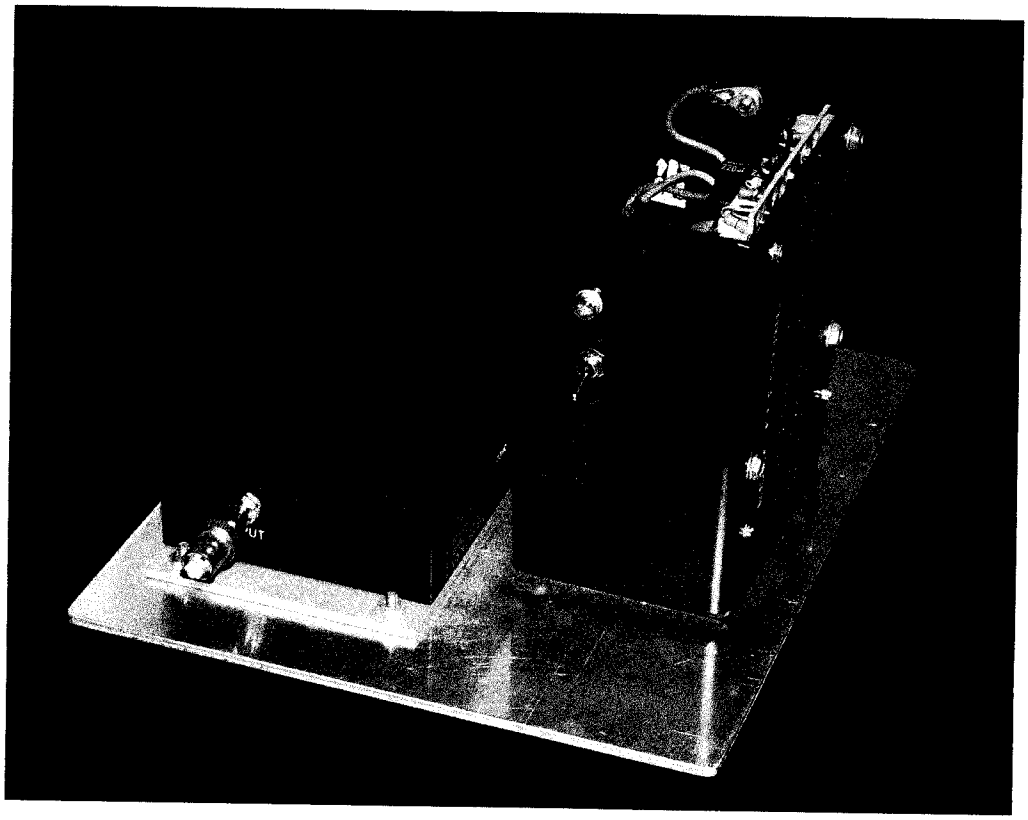

Figure 62 Example of a Preamplifier for the UHF Band

Some sacrifice in the noise figure for all preamplifiers was necessary in order to achieve a sufficiently high dynamic range for practical measurements. Noise figures of 6 to 12 dB are provided by the preamplifiers normally used compared to the approximately 2-dB noise figures achieved by low-dynamic-range units. Additional low-noise preamplifiers were provided for special measurements, but extreme care was taken in their use to avoid intermodulation problems.

The signal environment frequently contained a mixture of random impulses, signals with various formats, impulsive noise, and impulsive radio interference along with a few discrete-frequency signals. High-level impulsive signals, noise, and interference can result in the production of impulsive and broadband intermodulation noise. Precautions to identify instances of strong impulsive signals, noise, and interference are essential to avoid contamination of recorded data and the misleading results from such contamination.

A.1.3 Spectrum Analyzers

Two types were used to collect data in the field. The first type was the popular scanning spectrum analyzer commonly used to examine radio signals. The second type was the FFT type of spectrum analyzer, although all of the available FFT analyzers required the use of a linear frequency translator due to their base-band operation. Both types of spectrum analyzers were employed for field measurements, although most measurements were made with the scanning type.

The selection of an appropriate model of a scanning spectrum analyzer was a major matter, and a number of models were used over past years. While excellent modern digitally-controlled scanning spectrum analyzers are available, they were seldom used during field measurements for a variety of technical reasons. First, their dead time between scans (not specified by any of the manufacturers) was far too long to cope with the rapidly-changing signal and noise conditions found in real life. The dead time also significantly reduces the ability of a spectrum analyzer to receive and define the properties of intermittent signals, noise, and interference. In addition, the use of keypad or keyboard controls resulted in unacceptable time delays for changing the analyzer operating parameters to cope with time-varying signal, noise, and interference conditions. However, the newer digitally-controlled analyzers are preferred for the laboratory measurement of time-stable signals and noise or other similar special purpose measurement tasks.

The older knob-controlled spectrum analyzers were found to be more suitable for field-measurement purposes. The time delay between spans of the older scanning-type analyzers is considerably lower than that for the newer digitally-controlled units thus increasing their ability to detect and define intermittent and frequency varying emissions. The knob controls permit the rapid adjustment of instrumentation parameters to cope with the need to define time- and frequency-changing signal and noise conditions.

The old Hewlett Packard Model 141 Spectrum Analyzer with RF heads covering the frequency ranges of 0 to 110 MHz and 0 to 1250 MHz was found to be the best available model for measurements within its frequency-coverage ranges. The Hewlett Packard Model 8565A Spectrum Analyzer was found to be the best available analyzer for the measurement of time- and frequency-changing and intermittent emissions in the microwave bands. While the signal-handling dynamic range of these two models was somewhat lower than for newer models, the short dead times between spans and the ability to rapidly alter operating parameters outweighed the dynamic-range considerations. These analyzers were often modified for specific measurement tasks to improve dynamic range, provide an external synchronizing capability, and further reduce their dead time between scans.

Both spectrum analyzer models provide the ability to quickly change operating parameters such as the center frequency of a band under observation, the frequency span of that band, the scan time, and the measurement bandwidth. In addition, the analyzers could be quickly switched to operate in a zero-span mode similar to that of a

fixed-tuned receiver. The scanning process could be synchronized to external synchronizing sources to aid in the fine-scale definition of the temporal structure of some repetitive signals.

The dead time between scans was carefully measured and documented for each spectrum analyzer prior to its use in the field. This was done for two reasons.

First, transients and intermittent signals can, and will, occur during the dead time of a scanning analyzer, and such transients and intermittent signals will not be received. Also, portions of repetitive impulsive signals and noise will occur during the dead time and not be received. The probability of receiving an unknown transient is the quotient of the ratio of the scan time to the scan time plus dead time. Because of this the magnitude of the dead time compared to the scan time is a significant disadvantage of a scanning spectrum analyzer. It is essential that this ratio be known and be as low as possible to properly understand and interpret the results of field measurements.

Second, the dead time between scans influences the duration of the time-history axis used to define the temporal properties of signals and noise. This will be described in more detail in the following section.

A.1.4 Time-History Display

A Model 7200B 3-Axis Display is used to portray the time-history properties of signals and noise in real time. It has been used by students and staff of the Naval Postgraduate School for a number of thesis projects and other tasks. The display is completely slaved to the operation of a spectrum analyzer, thus only visually-related adjustments are provided on the instrument. The easiest way to demonstrate its presentation and capabilities is to review an example. Figure 63 shows an example of the presentation provided by a Model 7200 display. Two views of the same data are provided. The top view shows amplitude vs. frequency in a presentation similar to that provided by most spectrum analyzers. The bottom view provides a time-history presentation of the same data as shown in the upper view.

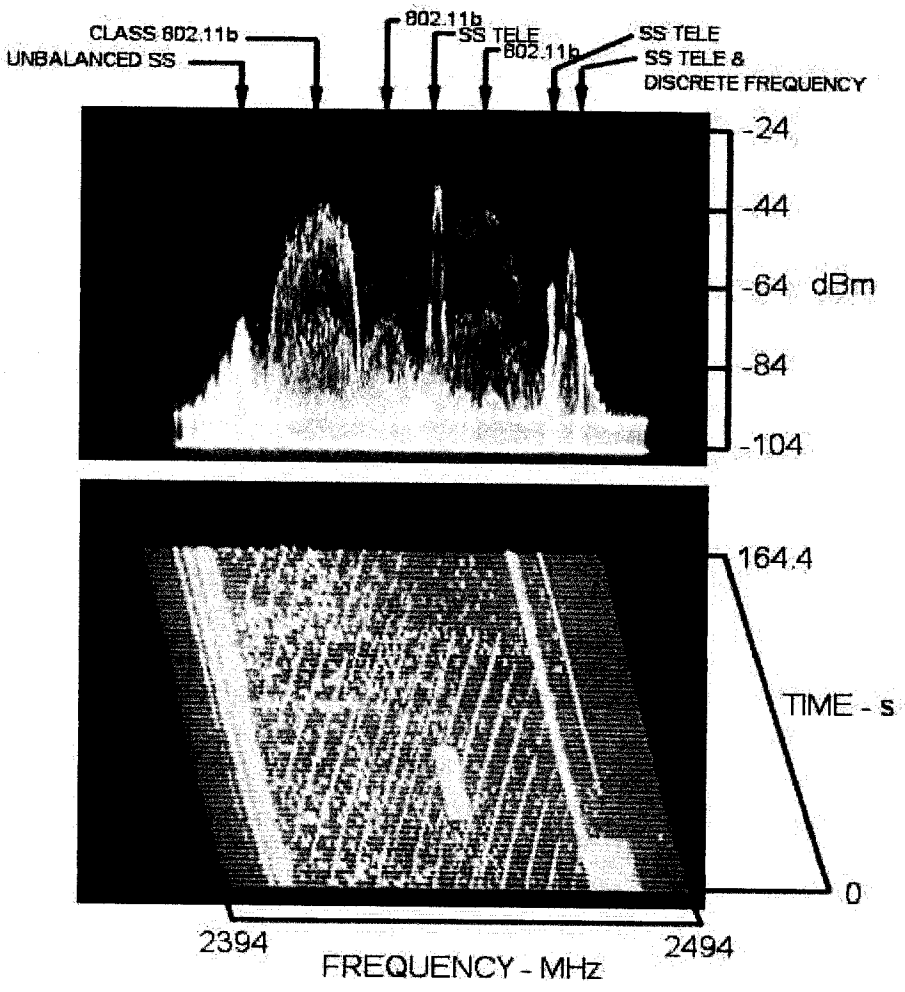

Figure 63 Example of Signals, Noise and Interference in the UHF Band

Information from each new scan of the spectrum analyzer is shown on the bottom line of the time-history presentation. Each new scan bumps all older scans up one line, and the oldest line at the top of the time-history presentation is discarded. This process occurs in real time. Prominent aspects of emissions in the example are identified by the annotation at the top of the amplitude-vs.-time view.

Several ways are available to enhance the time-history presentation of signals, noise, and interference. For example, the time axis can be slewed (or rotated); the time axis is slightly skewed to the left in the example to better show the slanting lines across the time-history view. The amplitude can be compressed; it is almost fully compressed in the time-history view and not compressed in the upper amplitude-vs.-frequency view of the same data. The elevation of the time-history view can be varied from 0 to 90 degrees; it is at zero degrees in the time-history view and at 90 degrees in the amplitude-vs.-frequency view. In addition, any set of 4, 8, 16, or 32 lines of the time-history view can be selected for a detailed line-by-line analysis of an emission. The amplitude threshold can be varied to minimize visual interference from low-level emissions. These features can be altered in real time to aid in portraying any desired feature. Any view can be frozen for a detailed examination or to photograph the two presentations, and the viewing enhancement controls also operate with a frozen view.

The slanting lines across the time-axis presentation are a result of receiving the broadband synchronizing pulses from an 802.11b access point as the spectrum analyzer scans across the bandwidth of the pulses. The scan time of the spectrum analyzer must be longer than the repetition period of the pulses, and the analyzer's IF bandwidth must be less than the spectral width of the pulse emission for this type of presentation. Since the data is obtained from a scanning filter, the time between impulses can be scaled from the horizontal axis which is a combination of frequency and scan time. The scan time of this axis is provided for each item of data, but it is not always added to the bottom horizontal axis to avoid excess material in the presentation.

The amplitude scale on Figure 63 refers to the amplitude of received signals at the output terminals of the antennas. The impact of receiver bandwidth on the amplitude of received signals is discussed later.

Synchronizing pulses from three 802.11b access points are shown in the time-history view. The clutter between the synchronizing pulses is from the 802.11b emissions of laptop computers using the networks as well as a few random pulses from other sources. Other signal formats are also shown in the two views such as the relatively narrow-band spread-spectrum signals from portable telephones..

The data in Figure 63 was obtained during a classroom session at the Naval Postgraduate School where wireless radio was extensively used as a classroom aid. Only the signal identified as "Class 802.11b" was associated with the classroom. All other signals came from other sources on the campus.

A.1.5 Data Recording

Until a few years ago, data was recorded by freezing the operation of the 7200B display and photographing the frozen view with a Tektronix Model C-5C Oscilloscope Camera using Polaroid film. Operating parameters were then written onto the back of each photograph. The pictures were trimmed and pasted onto white cardboard, and scales were manually added to the frequency, amplitude, and time axes. The resulting paste-ups were then scanned and recorded as a computer file. While this manual process was tedious, it provided excellent examples for the documentation of the results of field measurements.

The increasing price of Polaroid film in recent years eventually became a major cost of conducting field measurements. This resulted in the modification of the Tektronix camera enclosure to incorporate a small digital camera into the C-5C case. A USB cable connection between the digital camera and a laptop computer now provides a means to place examples of the two views from the time-history display directly onto the hard drive of a laptop in a standard .jpg format. The two views are subsequently combined into a single file, and the frequency, amplitude, and time scales are added to each set of views along with any desired annotation using a standard photo-processing program. The end result is a compressed .jpg file ready for direct insertion into the text of a report. This process eliminated the high cost of film and the cost of the manual graphics effort needed to format the Polaroid pictures.

A digital recording capability is built into Model 7200B display. This capability was seldom used since useful and effective digital data-processing techniques could not be applied to much of the data accumulated for this effort.

A.1.6 Data Calibration and Scaling

Comprehensive records are maintained for each item of data collected in the field. These records include the following items about each item of data.

Measurement Location
Picture Number
Date in yymmdd Format
Local Time
Center Frequency of Data
Frequency Span
Measurement Bandwidth
Scan Time in ms
Signal Source (Usually an Antenna ID)
Filter ID
Preamp Gain
RF Attenuator Setting
Signal Reference Level
Comments
Additional Special Comments

An abbreviated version of the above parameters is added below each item of formatted data as shown by the line of text at the bottom of Figure 63. Sufficient information is provided in this line to add amplitude, frequency, and time scales to the data and to reference each item of data to its source.

The amplitude scales in this document are calibrated in dBm to provide a convenient means to relate recorded data to commonly accepted spectrum analyzer calibration terms. Noise temperature has not been used as a measure of interference to the reception of a desired signal. This is because the term has not yet been defined sufficiently to describe the erratic time and frequency-varying conditions found in the wireless bands as well as the measurement bandwidth considerations.

The amplitude scales in this document show the peak level of signals, noise, and interference as received within the measurement bandwidth of the spectrum analyzer. The peak amplitude of any emission whose bandwidth is equal to or smaller than the measurement bandwidth can be determined directly from the amplitude scale shown on the right edge of the amplitude-vs.-frequency view. Impulsive signals and broadband signals with spectral content wider than the measurement bandwidth are always higher in amplitude than shown by the amplitude scale. This is because some of the spectral content is outside the measurement bandwidth.

An empirical curve has been generated by Hodge[14] to provide an approximate means to scale the amplitude of wide-band emissions to other than the measurement bandwidth. Figure 64 shows this curve along with a second curve for wideband Gaussian noise.

---

[14] James W. Hodge, ***A Comparison between Power-Line Noise Level Field Measurements and Man-Made Radio Noise Prediction Curves in the High Frequency Radio Band,*** MS Thesis, Naval Postgraduate School, Monterey, CA, December 1995

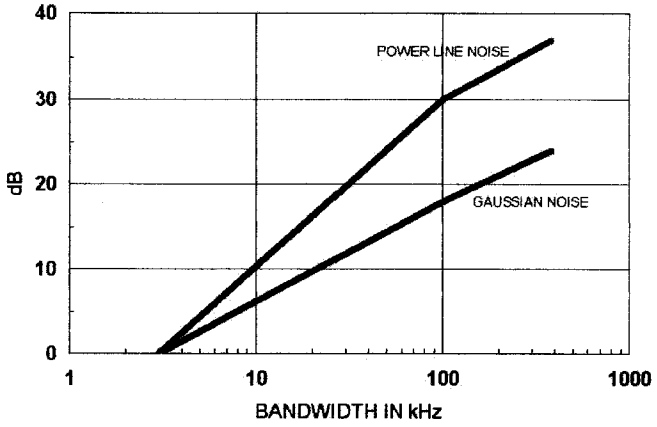

Figure 64 Bandwidth Compensation Plot

While the above Hodge curve was derived primarily from measurements of impulsive power-line noise in the HF and VHF bands, it has been shown to provide reasonable estimates for pulse emissions and impulsive noise and interference in the wireless bands. The curve is valid for receivers using Gaussian-shaped measurement bandwidths such as the bandwidth shapes used by many models of spectrum analyzers. To our knowledge similar curves have not been obtained for receivers with more rectangular IF bandpass filters.

Since the temporal structure of emissions in the wireless bands change significantly over brief intervals of time and with frequency, and are clearly non-Gaussian, one cannot provide a universal and acceptable way to define the average, root-mean-square, or other measures of amplitude other than at a selected time and for a specific small frequency band.

Finally, the duration of the time-history axis must also be determined to understand the variations of the emissions received over time and frequency. For a 60-line time-history display, the duration of the time axis, T(s), is determined by:

$$T(s) = [(\text{Scan Time in ms} + \text{Blanking Time in ms}) \times 60] / 1000$$

For a 120-line time-history display the duration of the time axis is:

$$T(s) = [(\text{Scan Time in ms} + \text{Blanking Time in ms}) \times 120] / 1000$$

The scan and blanking times are measured prior to each field use, and they are recorded along with other operating and site parameters. Tables 2 and 3 show the measured blanking times and the resulting duration of the time-history axis for two examples of instrumentation configurations. Since multiple sets of instrumentation are available, a similar chart is provided for each field measurement instrumentation configuration.

Table 2 Typical Calibration Data – NPS HP 141 #5

Scan Time/div ms	Total Scan Time ms	Free Run Scan + Blank ms	Free Run T(s) s	Line Sync Scan + Blank ms	Line Sync T(s) s
1	10	15.1	0.91	16.5	0.99
2	20	25.1	1.51	33.7	2.02
5	50	67.9	4.07	65.6	3.94
10	100	183.0	11.0	183.0	11.0
20	200	283.0	17.1	299.0	17.9
50	500	582.0	34.9	594.0	35.6
100	1000	1,082	64.9	1,096	65.8
200	2000	2,626	157.6	2,641	158.8
500	5000	5,628	337.7	5,632	337.9
1000(1 s.)	(10 s.)	10,624	637.4	10,632	637.9

Table 3 Typical Calibration Data – WRV HP 140

Scan Time/div ms	Total Scan Time ms	Free Run Scan + Blank ms	Free Run T(s) s	Line Sync Scan + Blank ms	Line Sync T(s) s
1	10	14.7	0.88	19.9	1.2
2	20	24.7	1.48	33.7	2.03
5	50	54.7	3.28	65.8	3.95
10	100	185.0	11.1	199.0	12.0
20	200	285.0	17.1	285.0	17.1
50	500	584.0	35.1	587.0	35.2
100	1000	1,084	65.0	1094	65.7
200	2000	2,084	125.0	2092	125.5
500	5000	5,084	305.0	3088	185.2
1000(1 s.)	(10 s.)	10,090	605.4	10,090	605.4

A.2 Instrumentation for Source Location and Identification

A variety of instrumentation and devices have been used to locate sources of noise and interference within the borders of a receiving site. For example, the instrumentation described in Section A1.1 can also be used with small probes to investigate on-site sources of noise and interference. In addition, additional instrumentation has been found to be highly useful, and examples of these are provided in this section. Some of these additional items are also used to investigate and identify sources of noise and interference external to a receiving site and their use is shown in reference 1 listed on page 1.

Figure 65 is a photograph of the Radar Engineers Model 242 portable noise receiver. It is tunable over the frequency range of 100 kHz to 1000 MHz, and it contains a small display of the temporal structure of examples of noise that is especially useful to portray the temporal structure of noise and interference that is synchronized to the power-line frequency. Data from this device is highly useful in relating and comparing the temporal structure of impulsive noise at a source location to that observed at the input terminals of a receiver.

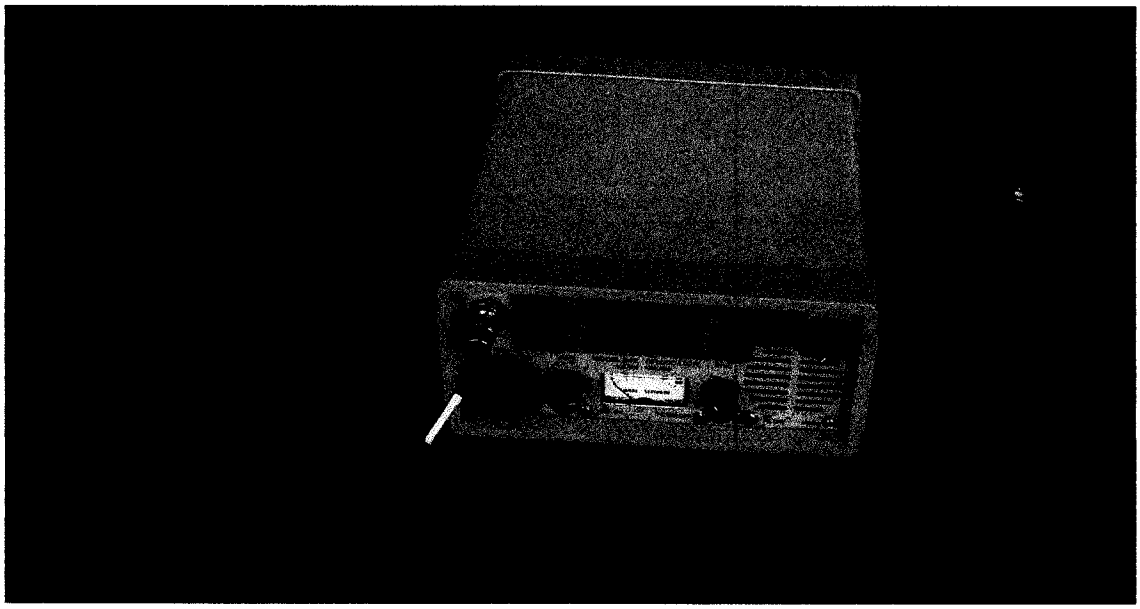

Figure 65 Radar Engineers Noise Receiver with Probe

The noise receiver is battery powered and can be carried to any convenient location. It can be used with a small whip antenna for general purpose or any other convenient source device. The above photograph shows it with a small probe that is used to pinpoint sources of unwanted emissions within a receiving or data-processing site.

The temporal structure of noise and interference observed on the Model 242 Noise Receiver can be recorded by photographing the display with a small conventional digital camera.

Figure 66 shows a Model F-70 Current Probe made by Fischer Custom Communications. It is used to examine and measure the level of spectral components of current flowing in any conductor up to about two inches in diameter. The probe provides a flat frequency response from 100 Hz up to 100 MHz, and its response can be calibrated down to about 30 Hz. The probe is matched to the 50-Ohm inputs of many amplifiers and spectrum analyzers. Spectral components of currents as low as 2μA can be measured with the use of a suitable low-noise preamplifier and a spectrum analyzer. This probe provides a means to make measurements of current to the low levels required to meet the limits provided in Table 1.

Figure 66 Model F-70 Current Probe

Caution must be employed with the use of the probe since many cases of noise and interference current are non-stationary. Thus, the amplitude of spectral components of current cannot always be accurately described with conventional measures of amplitude.

Figure 67 shows a Radar Engineers Model 245 Circuit Sniffer. This device is useful to detect the location of devices emitting unwanted broadband noise and interference from power-conversion sources. It is shown with its small whip antenna for general probing. It also contains a small magnetic-field sensor on the upper right corner of its case. This sensor is highly useful when scanning the circuit breakers of a power panel to identify which breaker feeds electric power to a power-conversion device or other noise source.

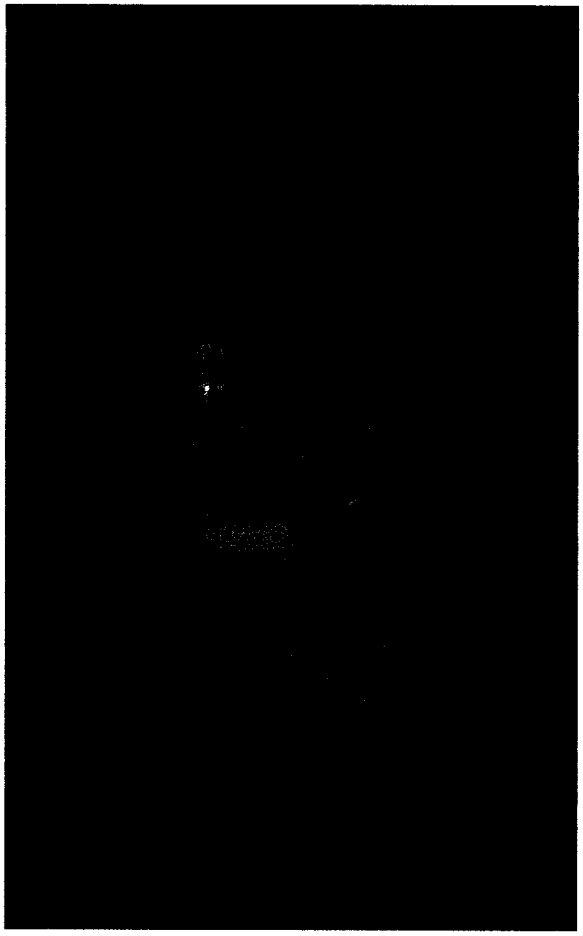

Figure 67 Circuit Sniffer Used to Locate On-Site Sources

This page is intentionally left blank

Initial Distribution List

	Copies
Defense Technical Information Center 8725 John J. Kingman Rd. Ft. Belvoir, VA 22060-6218	1
Dudley Knox Library, Code 013 Naval Postgraduate School Monterey, CA 93943-5100	2
Research Office, Code 09 Naval Postgraduate School Monterey, CA 93943-5138	1
Federal Communications Commission 445 12th St SW Washington .D.C. 20554 Attention: Julius Knapp, Deputy Chief, Office of Engineering and Technology	1
University of Kansas Center for Research 2385 Irving Hill Road Lawrence, Kansas 66045 Attention: Gary Minden	1
Naval Postgraduate School Electrical and Computer Engineering Department 833 Dyer Road Monterey, CA 93943 Attention: Mr. Andrew A. Parker Code EC/pk, Spanagel Hall	1
Dr. Richard W. Adler 870 E. Center St. Bountiful, UT 84010	1

Mr. George F. Munsch
160 County Road 375
San Antonio, TX 78253 — 1

USAINSCOM
IALO-E
8825 Beulah St
Fort Belvoir, VA 22060-5246
Attention: MS Anne Bilgihan — 1

Mr. Vil Arafilies
9542 Westwood Drive
Ellicott City, MD 21042 — 1

Reference and Interlibrary Loan Librarian
U.S. Department of Commerce
325 Broadway MC5
Boulder, CO 80305
Attention: Ms Carol J. Gocke — 1

Argon ST
12701 Fair Lakes Circle
Fairfax, VA 22033
Attention: Mr. Carlo Melnick — 1

Pennsylvania State University
Box 30
State College, PA 16804
Attention: Mr. Richard Groff — 1

Mr. Fred Horning
Radar Engineers, Inc.
9535 N.E. Colfax St.
Portland, OR 97220 — 1

Mr. Werner Graf
SRI International
333 Ravenswood Ave.
Menlo Park CA 94025 — 1

American Radio Relay League
225 Main Street
Newington, CT 06111-1494
Attention: Mr. Ed Hare

1

Mr. Marvin Loftness
115 West 20th St.
Olympia, WA 98501

1

Professor James K. Breakall
Pennsylvania State University
ECE Department
University Park, PA 16802

1

Mr. J. Mark Major
Southwest Research Institute
P.O. Drawer 28510
San Antonio, TX 78228-0510

1

Mr. Gregory Bragdon
DISA-JFCOM
Suite 200
1562 Mitscher Ave
Norfolk, VA 23511

1

Warrington Training Center
P.O. Box 700
Warrington, VA 20188
Attn: Station D (Robert Stone)

1

Attention: Jeff Blosser
7697 1st Street, Room 2
Tinker AFB, OK 73145

1

Mr Steve Colman
822 S. Waco St.
Van Alstyne, TX 75495

1

Mr. Stu Smeby
8780 Partridge Run Way
Bristow, VA 20136

1

Wilbur R. Vincent
1515 Shasta Drive, No. 1519
Davis, CA 95616

2

Mr. Eric Miller
Argon ST, Inc.
12701 Fair Lakes Circle
Fairfax, VA 22030

RADIO-FREQUENCY EMISSIONS FROM A SMALL WIND FARM

By Wilbur R. Vincent

INTRODUCTION

The Budweiser Brewery in Fairfield, California installed a large wind turbine for supplemental electric power in 2012. A second similar wind turbine was added in 2015. The location of the small wind farm, close to the home location of the instrumentation used to explore radio-frequency emissions from unusual sources, was convenient. In addition, roads in the near vicinity of the wind turbines with little traffic provided good locations to explore possible radio-frequency emissions from the wind farm.

Figure 1 shows a Google map of the area containing the wind turbines. The two yellow dots are adjacent to the base of the two wind turbines. The black slanting line from the bases of the wind turbines is their shadow. The main Budweiser facility is located north of the area shown on the map. Buried conductors carried electric power from the wind turbines to the Budweiser facility.

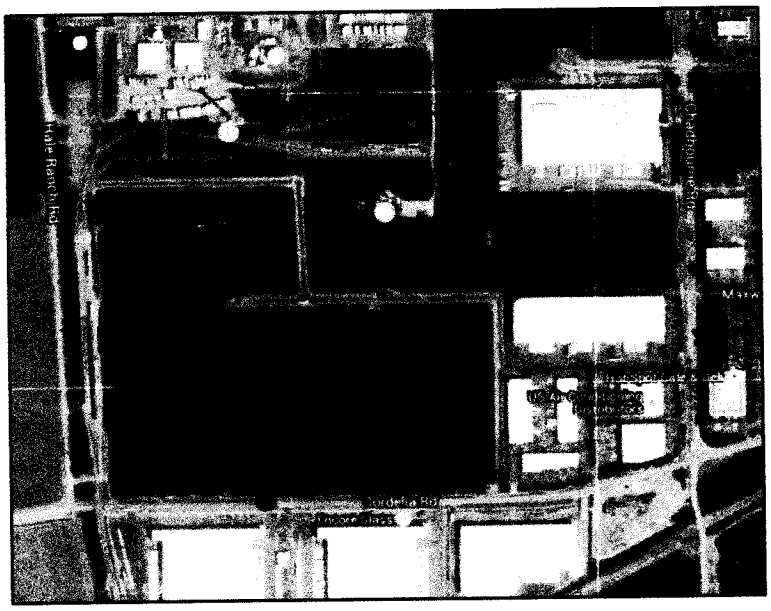

Figure 1 Overhead View of Windfarm

Initial tests were conducted from the single turbine located near the center of Figure 1 in April of 2012. These initial tests used an 8-ft whip as the receiving antenna. Additional measurements were made after the installation of the second turbine. The later tests were made at a more distant location south of the two turbines, where the red dot near the bottom of Figure 1 shows the location of most subsequent tests. A 17-ft antenna located 1713 feet from the nearest wind turbine and 2064 feet from the furthest wind turbine was used for the subsequent tests described in this paper. The paved road at this location provided access to nearby industrial facilities. A road barrier at the measurement location stopped all thru traffic and provided an excellent measurement location free of traffic.

A small solar farm is shown to the left of the original wind turbine. The solar farm was constructed in a depressed area with the solar elements at about surface level. All associated cables appear to be buried.

INSTRUMENTATION

A block diagram of the instrumentation used to collect the data provided in this document is shown in Figure 2.

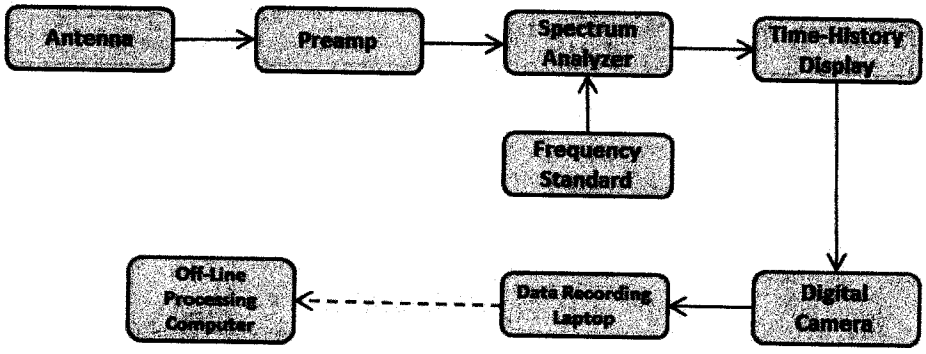

Figure 2 Block diagram of instrumentation

The instrumentation was developed specifically to investigate radio-interference problems at a variety of locations. It is described in detail in two handbooks prepared to assist others in the investigation of radio-interference problems. [1, 2, 3]

The antenna was a standard 17-ft collapsible vertical antenna mounted on a 2-ft by 2-ft aluminum plate. A bank of band-pass filters was available to suppress strong signals from transmitters in the HF International Broadcast bands sufficiently to avoid overloading the preamplifier. While available, the band-pass filter bank was not required during the daytime measurements of this effort, thus it is not shown on the block diagram. Daytime absorption of signals in the HF band reduced ambient signals to manageable levels.

The preamplifier was a high-dynamic-range unit previously used for the investigation of radio interference at receiving sites. The preamplifier provided a gain of 20 dB and a noise figure equivalent to that of a standard HF/VHF receiver. The preamplifier provided a minimum signal-level-detection capability of -128 to -130 dBm when using a 3-kHz Gaussian-shaped signal-detection bandwidth of 3 kHz.

The spectrum analyzer was a recently overhauled and calibrated HP Model 141. To improve the ability to set center and end-of-scan frequencies, a Global Specialties Model 4401 Frequency Standard was added to the measurement system to provide precise marker frequencies.

A Model 7200B Time-History Display was used to visually portray the real-time time-history temporal and spectral characteristics of received emissions and signals. Sixty successive scans of the spectrum analyzer are shown in either moving or fixed views. The azimuth, elevation,

---

[1] Wilbur R. Vincent, George F. Munsch, Richard W. Adler and Andrew A. Parker, *The Mitigation of Radio Noise from External Sources*, 6th Edition, May 2007, Naval Postgraduate School, Monterey CA

[2] Wilbur R. Vincent, George F. Munsch, Richard W. Adler and Andrew A. Parker, *The mitigation of Radio Noise and Interference from On-Site Sources*, November 2009, Naval Postgraduate School, Monterey CA

[3] References 1 and 2 are available to download at www.nps.edu/the mitigation of radio noise from external sources and www.nps.edu/the mitigation of radio noise and interference from on-site sources.

compression, freeze/unfreeze and threshold controls provide a means to optimize the visual view of received signals and interference.

A specially fabricated digital oscilloscope camera permits the recording of any fixed view of signals and interference, or a video of the real-time view of the time-history display.

An HP Model 8540 Elite-Book laptop is used to record fixed examples of data viewed on the time-history display, or videos of the moving time-history display as it collects data in real time. The laptop is equipped with all the software needed to produce finished examples of data collected in the field. A desktop computer is used to format final examples of data recorded in the field and to produce the documentation to complete this technical memorandum.

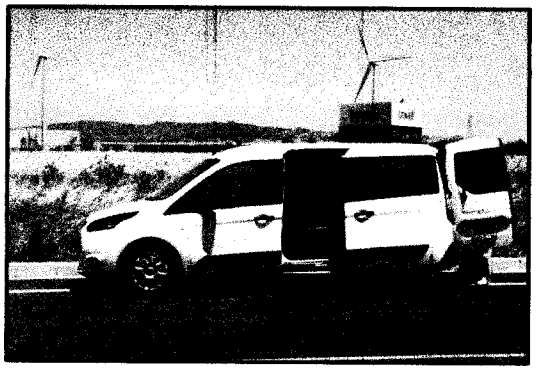

Figure 3 Instrumentation van at Location A

The field instrumentation is installed in, and operated from, a table in a small van. A Honda 2000 gasoline generator is included to provide electric power for the instrumentation. Figure 3 provides a photograph of the van containing the instrumentation while in operation at the Budweiser site. For these measurements, the van was parked at a temporary road-end barrier and opposite from a paved access driveway to local warehouses. The location provided an excellent line-of-sight path to the two wind turbines in the background.

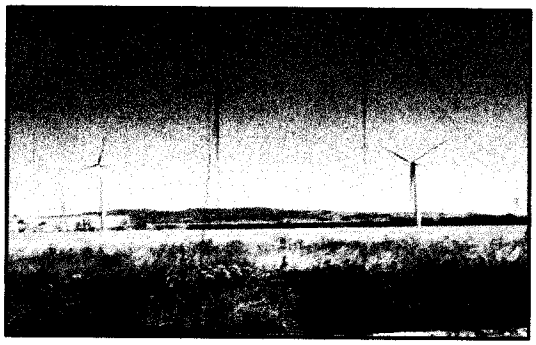

Figure 4 Antenna with wind turbines

Figure 4 shows the 17-ft-collapsible antenna with the two wind turbines in the background. The antenna is mounted on a 2-ft. by 2-ft. aluminum plate, and it was located about 60 ft. in front of the instrumentation van. A strong wind caused the flexible antenna to bend somewhat, and a bag of rocks was needed on the aluminum plate to keep the antenna upright.

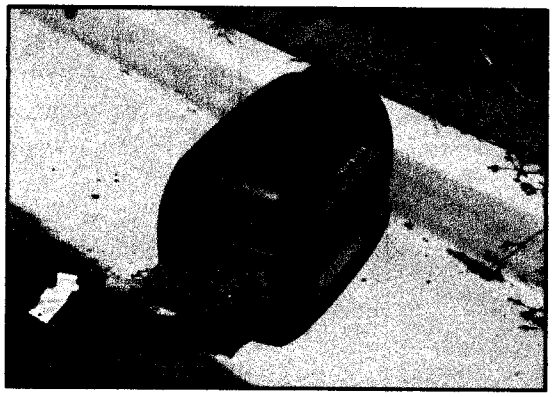

Figure 5 Honda Generator and Filter

Figure 5 shows the Honda generator used to provide instrumentation power at remote locations. The Honda 2000 Generator was located about 75 ft. to the rear of the instrumentation van. It also shows the power-line filter used to suppress impulsive electrical interference originating from the generator's solid-state dc-to-ac converter. Without the filter, the converter injects unwanted levels of impulsive current at HF frequencies into the power cord. The filter plugs into the 120-V output connector on the generator, and it reduces generator interference to undetectable levels by the instrumentation.

Fig

EXAMPLES OF DATA

The initial measurements using an 8-ft receiving antenna revealed some interesting details about the radio-frequency emissions from a single wind turbine. Figure 6 shows a typical pair of views of the same data where the top amplitude-vs.-frequency view shows distinctive peaks and nulls in wind turbine emanations over the lower half of the frequency range. These peaks and nulls appear to be related to the electrical height of the tall tubular supporting structure for the turbine, and they suggest that substantial levels of impulsive current and voltage in the HF band (3 to 30 MHz) are flowing on the support structure. Three fixed-frequency signals exceeded the level of the impulsive interference.

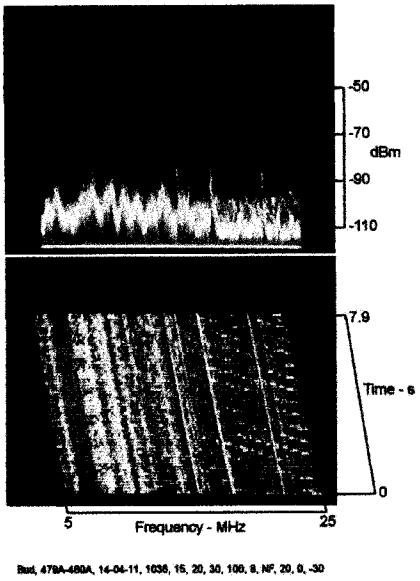

Figure 6 Wide Frequency Span of Emissions

The lower time-history view of Figure 6 suggests the presence of both widely-spaced impulses and closely-spaced impulses; however this view does not adequately describe either set. The source of the impulsive current is believed to be the dc-to-ac power converter associated with the turbine, where leakage from the converter allows impulsive current/voltage to appear on the support tower. The three fixed-frequency signals are the narrow lines parallel to the time-history axis.

The bottom view of Figure 7 shows how the amplitude variations of the emissions at 8.5 MHz varied over time. Six peaks and nulls in amplitude are shown over the 7.9 seconds of the measurement. These peaks and nulls were visually correlated with blade movement. As each of the three blades passed the tower, a 5- to 10-dB null in the emission amplitude occurred. This is a direct indication of a parasitic interaction between the moving turbine blades and the radiating tower.

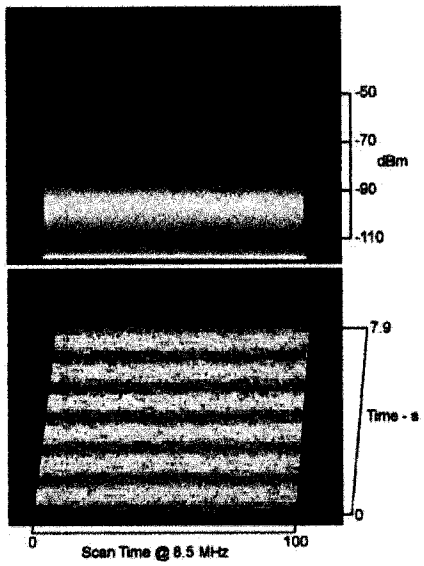

Figure 7 Peaks and nulls in the Emissions at 8.5 MHz

A re-examination of the time-history view of the Figure 6 also reveals amplitude modulation on the strong emission peak near the low end of the frequency range. This is the spectral component near the quarter-wavelength height of the tower, the frequency where maximum interaction would be expected. The amplitude of the emission peaks decrease as frequency increases.

These initial results indicate that a more complete investigation of the wind-turbine emanations would be in order, and additional measurements were conducted at a later date. The introduction of a second wind turbine at that location significantly altered the data in that two radiating devices were now present.

Two additional visits were made to the location shown at the red dot near the bottom of Figure 1. The first was on 27 June 2015 and the second was on 11 July 2015. Both visits were on a Saturday to minimize local traffic.

Examples of data from the first visit are presented below. Figure 8 shows two examples of ambient signals and emissions from the two wind turbines where the two examples cover different frequency ranges. The lower view shows a snapshot of a time-history view. The upper view shows the amplitude-vs.-frequency presentation of the same data as in the lower view.

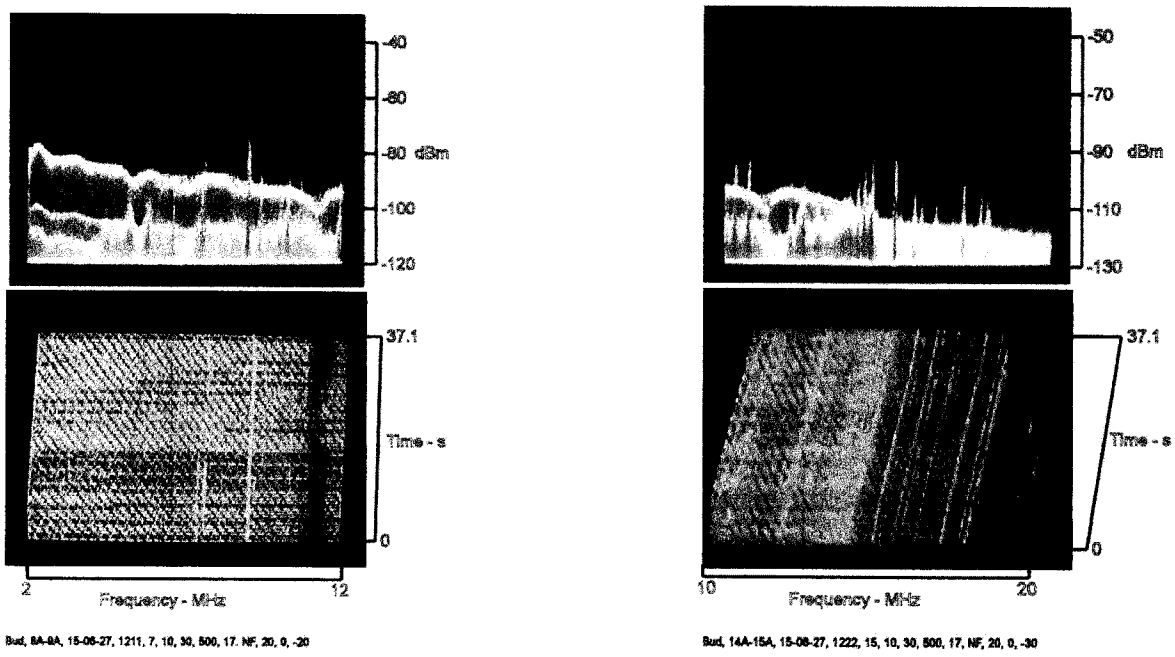

Figure 8 Examples of the Temporal and Spectral Structure of Emissions

In the left example, most signals in the 2- to 12-MHz frequency range are buried under wind-farm emissions. The one signal exceeding the emission level is a continuous signal at 10 MHz. The source of this signal was not identified until a later visit. In the right example, several high-level ambient signals in the 10- to 20-MHz frequency range exceed the wind-turbine emission level, but many signals from low-powered sources are buried under the emission level. The emission level fell below the ambient interference level at about 20 MHz, where the noise floor was determined by emissions from nearby industrial facilities.

The time-history presentation shows many closely-spaced bursts of noise during each scan of the analyzer (500 ms/scan) along with unusual variations in amplitude during the 37.1-second time shown. Both time-history views show variations in the temporal structure over time. Visual observations indicated that the variations are related to blade movement with respect to the wind-turbine towers. This was not fully examined during this series of measurements due to the difficulty of visually relating blade movement of two widely-separated wind turbines (having uncoordinated rotation speeds and blade positions) to the moving time-history view of the instrumentation.

The scan time of the analyzer was decreased to 100 ms, and the frequency span was reduced to 1 MHz, to provide an expanded view of the temporal structure of the emissions. Figure 9 shows the resulting increase in separation of the bands of noise. The slanting bands are because the analyzer-sweep process and the noise-generation process operate on separate and non-synchronized time bases. The spacing between primary bands is about 16.66 ms, the period of a 60-Hz power-line frequency. Each band of noise consists of several closely-spaced impulses. The wavy lines within the bands in the upper 1/3 of the time-history axis indicate the time base generating the impulses is slightly variable.

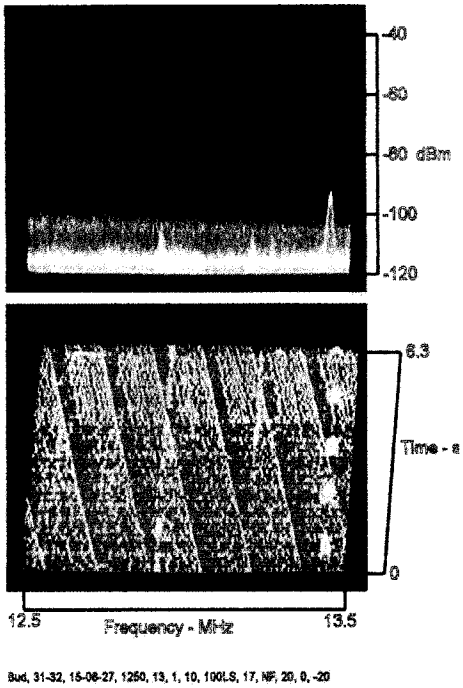

Figure 9 Increased Definition of Wind-Farm Emissions

A few fixed-frequency signals are parallel with the time-history axis, and a prominent on/off signal is shown near the upper end of the frequency scale. Its amplitude exceeded the level of the wind-turbine emissions.

A significant change in the temporal structure of the emission occurred about ¼ down from the top of the time-history view of Figure 9. Some aspect of the operation of the two wind turbines changed at this time.

A following visit was made to the measurement site on 11 July 2015, and the results were different. On this visit, the instrumentation was turned on at 11:30 am, and wind-farm emissions were not present; but there was no blade movement because of the lack of wind. Just before noon, a high-level burst of noise was noted. The burst was too brief to obtain a good record of its properties. The instrumentation was set to its free-run state, and it shortly recorded additional bursts of noise.

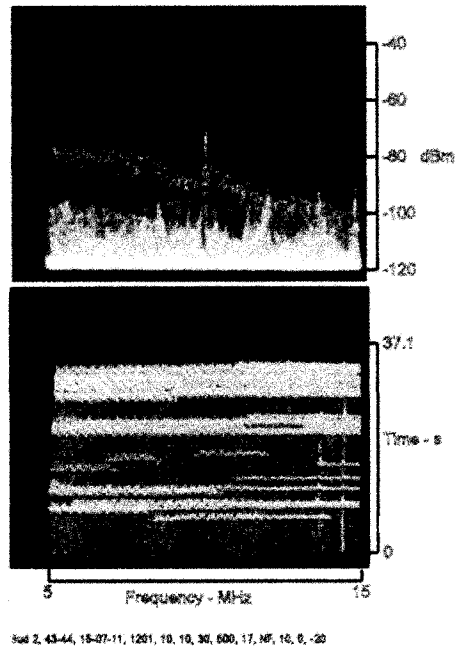

Figure 10 Erratic Emission Bursts, 5 to 10 MHz

Figure 10 shows an example of the erratic bursts of wind-turbine emissions observed at 12:01 pm LT. The longer burst of a few seconds duration at the top of the time-history view appeared first, followed by several shorter emission bursts. This was different from the continuous emissions of all previous measurements at the Budweiser facility.

The upper view of Figure 10 shows the amplitude of the emissions. A few signals are also present in this view, where most are below the level of the emissions. A single high-level signal at 10 MHz exceeded the emission amplitude and was very stable in amplitude. It did not fade over time like most signals in the high-frequency band. This signal is better shown in the next example, where its source is identified.

Figure 11 shows three short bursts of emissions received at 12:20, again over the 5- to 15-MHz frequency range. The lower view shows a weak signal at 10 MHz over the entire 10.7-second duration of the example. This weak signal was injected into the system from the frequency standard, and it was used to set the center frequency of the spectrum analyzer scan. The frequency-marker signal was purposely set low in amplitude.

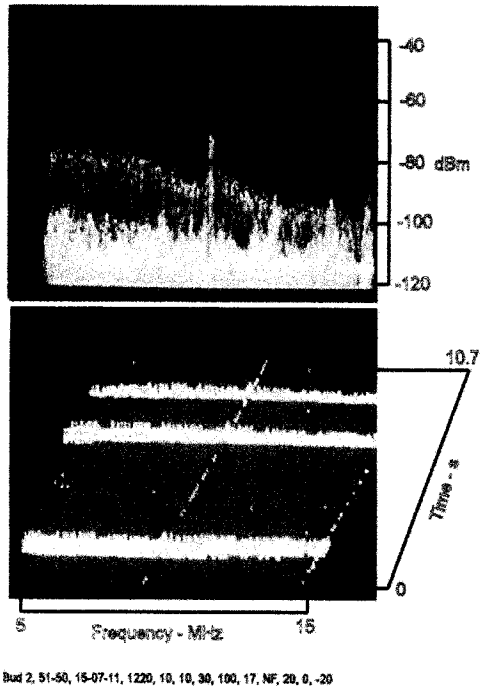

Bud 2, 51-50, 15-07-11, 1220, 10, 10, 30, 100, 17, NF, 20, 0, -20

Figure 11 Erratic Emissions, 5 to 10 MHz

A close examination of each burst in the time-history view of Figure 11 shows a strong signal at 10 MHz during each burst, although the highly-compressed amplitude of this view makes it somewhat difficult to identify this signal. This higher-level 10-MHz signal only occurred during each burst. The amplitude of this signal is shown in the upper amplitude-vs.-frequency view. It covered up the weak 10-MHz marker during each burst. The strong signal 10-MHz emission was associated with the operation of the turbine's dc-to-ac converter, and it probably originated from its time-base source.

Figure 12 shows an example of wind-farm emissions over the frequency range of 10 to 30 MHz. The burst durations seemed to increase over time although this is a subjective comment since short bursts also appeared at erratic times. The amplitude of the emissions fell below the ambient noise floor at about 27 MHz.

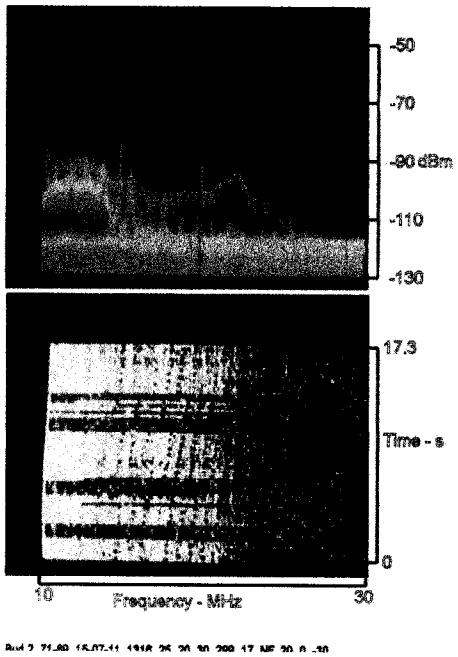

Figure 12 Erratic Emissions, 10 to 30 MHz

The prominent discrete-frequency signals exceeding the emissions at 15 and 20 MHz are also from the wind turbine. They also occurred only during emissions bursts. Of interest is that a fixed-frequency signal from the wind farm was not noted at 25 or 30 MHz.

Again, peaks and nulls in the amplitude of the emissions with frequency indicate resonance conditions from some combination of the source, the electrical length of the radiating tower and the electrical length of the receiving antenna.

The erratic bursts continued for several hours. While the duration and spacing of the bursts changed erratically, continuous operation of emissions was never observed during this second measurement period. This suggests that the wind turbines were probably operating on a power-demand mode during this second measurement time.

DISCUSSION

Each visit to the small Budweiser Wind Farm resulted in experiencing some new and unexpected aspect of radio-frequency emissions from that facility. Since the wind turbines themselves have not been examined, nor has its operator been contacted, the reasons for the differences are not known with certainty. One can speculate that the operators of the facility are improving its operation to meet their power-generation needs; resulting in occasional changes in the operation of the two wind turbines and in their radio-frequency emissions.

The data suggest that each turbine contains a power converter to synchronize its produced power to the frequency of the local-utility power-distribution system. Furthermore, the converters inject significant levels of high-frequency current and voltage onto the large vertical towers supporting the wind turbines. The two tall towers (over 100-feet) are efficient vertical radiators of the impressed high-frequency current and voltage. The modulation of emission amplitude as a blade moves across a tower supports this finding. The blade modulation and the changing power-demand aspects of the emissions results in erratic-appearing time-history data.

The presence of very strong 10-, 15- and 20-MHz signals emanating from the wind-farm towers was unexpected. The data indicate that these wind-farm emissions will interfere with the reception of standard-frequency signals from WWV and WWVH (*the National Institute of Standards and Technology WWV/WWVH radio station*) at any place within several miles of the facility.

The intermittent broad-band emissions suggest that the site was operating in a "Power-Demand" mode during the last visit. As electric power is needed, the tower inverters are turned on and then off. Of interest is the apparent instant synchronization of the inverters with the power grid. At other wind-farms, the impulse period from wind-turbine converters have been observed to vary for a few seconds, until the period of the power grid is reached.

No high-frequency emissions were noted from the nearby solar farm (see Figure 1), indicating that the solar-system power-conversion devices were well shielded. The strong high-frequency emissions from the wind turbines indicate that shielding techniques were not employed in the wind-turbine converters to minimize radio-interference issues. All high-frequency band allocated to the amateur radio service encountered severe radio interference.

A survey of the technical literature did not find other published information about high-frequency emissions from wind farms.

The instrumentation used in this investigation was able to cope with and define the primary properties of both time-stable emissions and time-erratic emissions. The later cannot be defined by conventional radio-noise-measuring equipment. This included the ability to define the spectral and temporal structure of the interference in sufficient detail to identify the source of the emission as two independent power-conversion devices employing switching technology.

CONCLUSIONS

Of concern is that the Budweiser wind farm, or any other similar farm, emits very high levels of radio interference that will adversely impact the performance of any high-frequency radio-receiving facility located within many miles of the wind farm. While the Budweiser facility was not of primary concern because of its location in a suburban area, it provided a convenient test bed for the effort described in this paper.

Of importance is that the emission-amplitude values provided in this memorandum were collected from a 17-ft-vertical antenna without ground radials. Most high-frequency receiving sites will have antennas that are much higher, more efficient, and with much more gain, than the collection antenna used to obtain the data shown. Thus the amplitude values provided in this paper, even though disturbingly high, must be considered to be very conservative. Also, there remains the very real possibility of wind-farm radio interference to overhead aircraft. This important possibility has not been explored.

Of interest is that radio-frequency emissions were not detected from the nearby solar farm, even though it was within line of sight from the instrumentation's antenna. The solar farm apparently employs a power-conversion device designed to minimize radio-frequency emissions. Radio interference from the power converters associated with the Budweiser Wind Farm could probably be substantially reduced if its converters were properly shielded and with filters added to all shield-penetrating conductors.

ABSTRACT

Radio Interference in the high-frequency band produced by a small wind farm was investigated. The temporal and spectral properties of the interference indicate the source is the power-conversion devices associated with each of the two wind turbines at the site. Both continuous-interference and intermittent-interference conditions were noted, suggesting the turbines operated in a power-demand mode, where interference was produced only when power was needed. In addition, strong discrete-frequency emissions were noted on 10, 15 and 20 MHz, indicating the presence of a frequency-reference source for synchronization with utility power.